Interfaces Free Bound. (Online first)
DOI 10.4171/IFB/493

Published by EMS Press

A convergent finite element algorithm for mean curvature flow in arbitrary codimension

Tim Binz and Balázs Kovács

Abstract. Optimal-order uniform-in-time H^1-norm error estimates are given for semi- and full discretizations of mean curvature flow of surfaces in arbitrarily high codimension. The proposed and studied numerical method is based on a parabolic system coupling the surface flow to evolution equations for the mean curvature vector and for the orthogonal projection onto the tangent space. The algorithm uses evolving surface finite elements and linearly implicit backward difference formulas. This numerical method admits a convergence analysis in the case of finite elements of polynomial degree at least 2 and backward difference formulas of orders 2 to 5. Numerical experiments in codimension 2 illustrate and complement our theoretical results.

1. Introduction

In this paper we prove semi- and fully discrete error bounds of a numerical algorithm for the evolution of a closed m-dimensional surface $\Gamma(t) \subset \mathbb{R}^n$ evolving under mean curvature flow of *arbitrary codimension*, with a particular interest in codimension at least 2.

The goal of the paper is to derive and analyze an algorithm for (high codimension) mean curvature flow. Our algorithm is based on the numerical approximation of a *nonlinear* parabolic equation system coupling the velocity law to evolution equations, for the mean curvature vector $\vec{H}$ and the orthogonal projection onto the tangent space π, along the flow. This is a similar approach to that of recent work for the numerical analysis of mean curvature flow [28], which first utilized such an approach using similar evolution equations for the (scalar) mean curvature and surface normal. For the numerical analysis of other geometric flows using this approach, see [13, 29, 30].

Similarly, as Huisken [26] did for codimension 1 mean curvature flow, in higher codimension Andrews and Baker [7] have derived numerous geometric evolution equations for various geometric quantities; see [39] as well. They used them to show existence of a unique smooth solution (with suitable initial value), which converges to a point in finite time. For mean curvature flow in arbitrary codimension (and dimension), we derive here evolution equations for the mean curvature vector $\vec{H}$ and the orthogonal projection π

2020 Mathematics Subject Classification. Primary 35R01; Secondary 53E10, 65M12, 65M15, 65M60.
Keywords. Mean curvature flow, higher codimension, evolving surface finite elements, backward difference formulas, error estimates.

onto the tangent space, which (to our knowledge) are not yet known in the literature. Until the present work, it was also not evident that these evolution equations for $\vec{H}$ and π form a closed system that does not involve further geometric quantities.

We now give a brief overview of mean curvature flow in higher codimension.

In two papers [3, 4], Altschuler and Grayson have proved the first results for curves in $\mathbb{R}^3$—namely that, unlike with planar curves, singularities may occur in finite time. Ambrosio and Soner [5, 6] have studied high codimension mean curvature flow using a level set approach. Andrews and Baker [7] have proved that submanifolds sufficiently close to the round sphere smoothly collapse to round points in finite time and have proved pinching estimates. They derive evolution equations for geometric quantities along the flow, similar to [26] in codimension 1, but have not derived the closed system of evolution equations derived and used in this paper. These pinching estimates were greatly refined by Naff in [36]. Ancient solutions were recently studied by Lynch and Nguyen [34]. In the survey article [39], Smoczyk presents results on short-time existence and uniqueness, long-time existence and convergence, and singularities. The survey-type article by Wang [40] collects several theorems on regularity, global existence, and convergence; see also [41].

We also give a literature overview on numerical methods for curve shortening and mean curvature flow in *codimension at least* 2 (while only giving a brief outlook on other flows):

Following the ideas of Dziuk [20] for mean curvature flow, Dziuk [21] and Deckelnick and Dziuk [15] have both proposed and analyzed finite element algorithms for curve shortening flow for curves possibly in higher codimension and have proved semi-discrete $L^\infty(L^2)$- and $L^2(H^1)$-norm error estimates. We note here that the original algorithm [20] works for high-codimension *surfaces*; however, convergence results were not yet proven. Carlini, Falcone, and Ferretti [14] proposed a semi-Lagrangian scheme for curve shortening flow in codimension 2 (i.e., closed curves in $\mathbb{R}^3$), and have analyzed its (conditional) consistency. Pozzi proposed a numerical method for anisotropic curve shortening and mean curvature flow in higher codimension in [37, 38], and proved semi-discrete error estimates for curves in arbitrary codimension. Barrett, Garcke, and Nürnberg [10] proposed numerical algorithms—allowing tangential movements—for gradient flows (including curve shortening and Willmore flow) for closed curves in $\mathbb{R}^n$ ($n \geq 2$). In [11] they discretized high-order flows for plane and space curves. Dörfler and Nürnberg [18] have proposed finite element discretizations for gradient flows for general curvature energies of space curves. A tangentially redistributing scheme for 3-dimensional curve evolutions was proposed in [35].

Apart from the convergence results for *curves in* $\mathbb{R}^n$ by Dziuk [21], Deckelnick and Dziuk [15], and Pozzi [37], we are not aware of any convergence results for mean curvature flow in *high codimension*.

The newly derived non-linear geometric evolution equations for the mean curvature vector $\vec{H}$ and orthogonal projection π are coupled with the velocity law $v = \vec{H}$ and the ordinary differential equation (ODE) $\dot{X} = v \circ X$ describing the surface evolution. This

geometric coupled system is then discretized using evolving surface finite elements (of degree at least 2) and using linearly implicit backward difference formulas (of order 2 to 5), under a mild step size restriction.

We prove optimal-order time-uniform H^1-norm semi- and fully discrete error estimates for mean curvature flow in arbitrary codimension and dimension, utilizing the newly derived geometric coupled system, for the surface position X, the velocity v, and the geometric quantities $\vec{H}, \pi$. The functional-analytic setting for the spatial semi-discrete coupled system of mean curvature flow in arbitrary codimension is fundamentally different from the one for mean curvature flow [28]. Still, the matrix–vector formulations of their respective semi-discretizations formally coincide. We regard this as an advantage of our algorithm. They both use the same mass and stiffness matrices with different block-sizes, but the non-linear terms are more complicated than in [28]; however, both are locally Lipschitz continuous. Due to this purely formal analogy of the matrix–vector formulations, the convergence proofs for arbitrary codimension mean curvature flow also formally coincide with the respective proofs in [28] for mean curvature flow. More precisely, since the non-linear terms are locally Lipschitz, the stability proofs of [28] directly apply to the present case as well. Consistency proofs are shown using similar arguments.

Arguably, for *curves*, the algorithm proposed here is more complicated to implement than the methods of Dziuk [21] and Deckelnick and Dziuk [15]; however, the algorithm proposed here comes with a convergence analysis for *surfaces*.

The paper is organized as follows: Section 2 introduces basic notations for arbitrary codimension submanifolds and contains the main technical results of the paper, which consist in deriving the evolution equations for $\vec{H}$ and π. Section 3 contains the evolving surface finite element spatial semi-discretization, and the corresponding matrix–vector formulation, and discusses its relation to the matrix–vector formulation of mean curvature flow [28]. Section 4 presents the linearly implicit backward differentiation formulas. Section 5 contains the main results of the paper—namely, semi- and fully discrete error bounds. Section 6 reports on a large number of numerical experiments to illustrate and complement our theoretical results, including convergence tests and comparisons with Dziuk's algorithm [21], and presents some examples from the literature.

2. Evolution equations for mean curvature flow

2.1. Basic notions and notation

We start by introducing some basic concepts and notations.

We consider an evolving m-dimensional ($m = 1, 2, 3$) closed submanifold $\Gamma[X] \subset \mathbb{R}^n$, that is, an m-dimensional submanifold in $\mathbb{R}^n$ of codimension $n - m$. In this paper we allow submanifolds of arbitrary codimension $n - m \geq 1$.

The m-dimensional submanifold $\Gamma[X]$ is given as the image

$$\Gamma[X] = \Gamma[X(\cdot, t)] = \big\{X(p, t) \mid p \in \Gamma^0\big\}$$

of a smooth mapping $X : \Gamma^0 \times [0,T] \to \mathbb{R}^n$ of an initial submanifold Γ^0 such that $X(\cdot,t)$ is an embedding for every t, and $X(p,0) = p$. Here, the initial submanifold $\Gamma^0 \subset \mathbb{R}^n$ is smooth and of dimension m. In view of the subsequent numerical discretization, it is convenient to think of $X(p,t)$ as the position at time t of a moving particle with label p, and of $\Gamma[X]$ as a collection of such particles. This approach is similar to the one in [28].

The *velocity* $v(x,t) \in \mathbb{R}^n$ at a point $x = X(p,t) \in \Gamma[X(\cdot,t)]$ equals

$$\partial_t X(p,t) = v(X(p,t),t). \tag{2.1}$$

For a known velocity field v, the position $X(p,t)$ at time t of the particle with label p is obtained by solving the ordinary differential equation in (2.1) from 0 to t for a fixed p.

For a function $u(x,t)$ ($x \in \Gamma[X]$, $0 \le t \le T$), we denote the *material derivative* (with respect to the parametrization X) as

$$\partial^\bullet u(x,t) = \frac{\mathrm{d}}{\mathrm{d}t}\, u(X(p,t),t) \quad \text{for} \quad x = X(p,t).$$

On a regular submanifold, we denote by $g_{ij} = \partial_i X \cdot \partial_j X = \sum_{\mu=1}^n \partial_i X_\mu \partial_j X_\mu$ ($i,j = 1,\dots,m$) the induced metric, where X denotes the local parametrization of the surface Γ. We denote its inverse by (g^{ij}). Moreover, we denote the second fundamental form by

$$A(x) = (A_{ij}(x))_{i,j=1}^m = \big((\partial_i \partial_j X(p,t))^\perp\big)_{i,j=1}^m = (\partial_i \partial_j X - \Gamma_{ij}^k \partial_k X)_{i,j=1}^m \in (\mathbb{R}^n)^{m\times m}.$$

Here, $^\perp$ denotes the orthogonal projection to the orthogonal complement of the tangent space of $\Gamma[X]$ at $x = X(p,t)$.

Furthermore, the *mean curvature vector* is the trace of the Weingarten map, that is,

$$\vec{H} = g^{ij} A_{ij} = (g^{ij} \partial_i \partial_j X)^\perp = g^{ij} \partial_i \partial_j X - g^{ij} \Gamma_{ij}^k \partial_k X \in \mathbb{R}^n;$$

in other words, we use the sign convention that for a sphere of radius R, the mean curvature vector $\vec{H}$ points inwards and has length m/R.

For every $x \in \Gamma[X]$, we denote the *orthogonal projection* from $\mathbb{R}^n$ to the tangent space of the submanifold $\Gamma[X(\cdot,t)]$, at the point $x = X(p,t)$, by

$$\pi(x) = g^{ij} \partial_i X \otimes \partial_j X \in \mathbb{R}^{n\times n}.$$

On any regular submanifold $\Gamma \subset \mathbb{R}^n$, the *tangential gradient* $\nabla_\Gamma u : \Gamma \to \mathbb{R}^n$ of a function $u : \Gamma \to \mathbb{R}$ is given by $\nabla_\Gamma u := g^{ij}\, \partial_i u\, \partial_j X$, and in the case of a vector-valued function $u = (u_1,\dots,u_n)^T : \Gamma \to \mathbb{R}^n$, we define $\nabla_\Gamma u = (\nabla_\Gamma u_1, \dots, \nabla_\Gamma u_n)$ componentwise, that is, we use the convention that the gradient of u has the gradient of the components as column vectors. We denote by $\Delta_\Gamma u = \nabla_\Gamma \cdot \nabla_\Gamma u$ the *Laplace–Beltrami operator* applied to u, so that on a closed surface we have $\int_\Gamma \Delta_\Gamma u\, v = -\int_\Gamma \nabla_\Gamma u \cdot \nabla_\Gamma v$ (cf. [23]).

2.2. Evolution equations for orthogonal projection and mean curvature vector of a submanifold evolving under mean curvature flow

Mean curvature flow (in arbitrary codimension) sets the velocity (see (2.1)) of the submanifold $\Gamma[X]$ to

$$v = \vec{H}. \tag{2.2}$$

For geometric surface flows (see, e.g., [26]), it is known that the geometric quantities satisfy evolution equations along the flow. The algorithm here is based on parabolic partial differential equations for the mean curvature vector $\vec{H}$ and the projection π, which are derived in the following result:

Lemma 2.1. *For a regular m-dimensional submanifold $\Gamma[X] \subset \mathbb{R}^n$ moving under mean curvature flow in codimension $n-m$, the orthogonal projection π and the mean curvature vector $\vec{H}$ satisfy*

$$\partial^\bullet \pi = \Delta_{\Gamma[X]} \pi + f_1(\pi), \tag{2.3a}$$

$$\partial^\bullet \vec{H} = \Delta_{\Gamma[X]} \vec{H} + f_2(\pi, \vec{H}), \tag{2.3b}$$

where the Laplace–Beltrami operator is understood componentwise. The non-linear terms are given componentwise, for $\alpha, \beta = 1, \dots, n$, by

$$\begin{aligned} f_1(\pi)_{\alpha\beta} &= 2 \sum_{\mu=1}^{n} \nabla_{\Gamma[X]} \pi_{\alpha\mu} \cdot \nabla_{\Gamma[X]} \pi_{\beta\mu} - 4 \sum_{\mu,\kappa=1}^{n} \pi_{\mu\kappa} \nabla_{\Gamma[X]} \pi_{\alpha\mu} \cdot \nabla_{\Gamma[X]} \pi_{\beta\kappa}, \\ f_2(\pi, H)_\alpha &= 2 \sum_{\mu=1}^{n} \nabla_{\Gamma[X]} \pi_{\alpha\mu} \cdot \nabla_{\Gamma[X]} H_\mu + 4 \sum_{\mu,\kappa=1}^{n} \nabla_{\Gamma[X]} \pi_{\alpha\mu} \cdot \nabla_{\Gamma[X]} \pi_{\mu\kappa} H_\kappa. \end{aligned} \tag{2.4}$$

Proof. The lemma is proved in Appendix A, in order for the paper to avoid local definitions as much as possible. The result follows from Lemmas A.6 and A.8, in a differential geometric setting using calculations in geodesic normal coordinates. ∎

These equations are formally the same as the analogous ones for mean curvature flow (the normal vector and mean curvature); see [26], or [28, (2.4) and (2.5)]. The non-linear terms are, however, more complicated.

In the case of codimension 1, we have $A_{ij} = -h_{ij}\nu$ and the mean curvature vector $\vec{H} = -\operatorname{tr}(h)\nu$, where h_{ij} denotes the second fundamental form and ν the outer unit normal. Furthermore, $\operatorname{tr}(h)$ is the scalar mean curvature. In this case, the orthogonal projection is given by $\pi_{\alpha\beta} = \delta_{\alpha\beta} - \nu_\alpha \nu_\beta$. Using the identities

$$\begin{aligned} \sum_{\mu=1}^{n} \nabla_{\Gamma[X]} \pi_{\alpha\mu} \cdot \nabla_{\Gamma[X]} H_\mu &= \sum_{\mu=1}^{n} g^{kl} \partial_k \pi_{\alpha\mu} \partial_l H_\mu \\ &= \sum_{\mu=1}^{n} g^{kl} (\nu_\alpha \partial_k \nu_\mu + \nu_\mu \partial_k \nu_\alpha)(\partial_l \operatorname{tr}(h) \nu_\mu + \operatorname{tr} \partial_l \nu_\mu) \\ &= g^{kl} \partial_l \operatorname{tr}(h) \partial_k \nu_\alpha + |h|^2 \operatorname{tr}(h) \nu_\alpha \end{aligned}$$

and

$$\sum_{\mu,\kappa=1}^{n} \nabla_{\Gamma[X]}\pi_{\alpha\mu} \cdot \nabla_{\Gamma[X]}\pi_{\mu\kappa} H_\kappa = \sum_{\mu,\kappa=1}^{n} g^{kl}\partial_k \pi_{\alpha\mu}\partial_l \pi_{\mu\kappa} H_\kappa$$
$$= -\sum_{\kappa=1}^{n} (g^{kl}\partial_k \nu_\alpha \partial_l \nu_\mu + |h|^2 \nu_\alpha \nu_\mu)\operatorname{tr}(h)\nu_\alpha,$$

as well as $\partial_k \nu = h_k^l \partial_l X$, we obtain from (2.3b) and (2.4) the evolution equation of the mean curvature vector:

$$\begin{aligned}\partial^\bullet \vec{H} &= \Delta_{\Gamma[X]}\vec{H} - 2|h|^2 \operatorname{tr}(h)\nu + 2g^{ij}g^{kl}\partial_i \operatorname{tr}(h) h_{jk}\partial_l X \\ &= \Delta_{\Gamma[X]}\vec{H} + 2|h|^2\vec{H} + 2(\nabla_{\Gamma[X]}\operatorname{tr}(h)) \cdot \nabla_{\Gamma[X]}\nu. \end{aligned} \tag{2.5}$$

Combining the evolution equations of the normal vector and mean curvature in [26] (see also [28, (2.4) and (2.5)]), we obtain equation (2.5) by the product rule.

2.3. A coupled system for mean curvature flow

The evolution of a submanifold of dimension m in codimension $n - m \geq 1$ evolving by mean curvature flow is then governed by coupled system (2.2), (2.3a)–(2.3b) together with ODE (2.1). The numerical method is based on the weak form of the above coupled system, which reads:

$$\begin{aligned} \nu &= \vec{H}, \\ \int_{\Gamma[X]} \partial^\bullet \pi \cdot \varphi^\pi + \int_{\Gamma[X]} \nabla_{\Gamma[X]}\pi \cdot \nabla_{\Gamma[X]}\varphi^\pi &= \int_{\Gamma[X]} f_1(\pi)\cdot\varphi^\pi, \\ \int_{\Gamma[X]} \partial^\bullet \vec{H} \cdot \varphi^{\vec{H}} + \int_{\Gamma[X]} \nabla_{\Gamma[X]}\vec{H} \cdot \nabla_{\Gamma[X]}\varphi^{\vec{H}} &= \int_{\Gamma[X]} f_2(\pi,\vec{H})\cdot\varphi^{\vec{H}}, \\ \text{together with the ODE} \quad \partial_t X &= v \circ X, \end{aligned} \tag{2.6}$$

for all test functions $\varphi^\pi \in H^1(\Gamma[X])^{n\times n}$ and $\varphi^{\vec{H}} \in H^1(\Gamma[X])^n$. This system is complemented by the initial data for X^0, π^0, and $\vec{H}^0$.

For simplicity, by $\cdot$ we denote both the Euclidean scalar product for vectors and the Frobenius inner product for matrices (i.e., the Euclidean product with an arbitrary vectorization).

We now directly compare the weak formulation of the coupled geometric system for mean curvature flow in codimension 1 derived in [28] (in particular, see [28, (2.6)]): Find the velocity v, scalar mean curvature H, outward unit normal vector ν, and the paramet-

rization X such that the following system holds:

$$\begin{aligned}
&\int_{\Gamma[X]} \nabla_{\Gamma[X]} v \cdot \nabla_{\Gamma[X]} \varphi^v + \int_{\Gamma[X]} v \cdot \varphi^v \\
&\quad = -\int_{\Gamma[X]} \nabla_{\Gamma[X]} (H\nu) \cdot \nabla_{\Gamma[X]} \varphi^v - \int_{\Gamma[X]} H\nu \cdot \varphi^v, \\
&\int_{\Gamma[X]} \partial^\bullet \nu \cdot \varphi^\nu + \int_{\Gamma[X]} \nabla_{\Gamma[X]} \nu \cdot \nabla_{\Gamma[X]} \varphi^\nu = \int_{\Gamma[X]} |\nabla_{\Gamma[X]} \nu|^2 \, \nu \cdot \varphi^\nu, \qquad (2.7) \\
&\int_{\Gamma[X]} \partial^\bullet H \, \varphi^H + \int_{\Gamma[X]} \nabla_{\Gamma[X]} H \cdot \nabla_{\Gamma[X]} \varphi^H = \int_{\Gamma[X]} |\nabla_{\Gamma[X]} \nu|^2 \, H \, \varphi^H, \\
&\qquad \text{together with the ODE} \quad \partial_t X = v \circ X,
\end{aligned}$$

for all test functions $\varphi^v \in H^1(\Gamma[X])^3$, $\varphi^\nu \in H^1(\Gamma[X])^3$, and $\varphi^H \in H^1(\Gamma[X])$. This system is complemented by the initial data X^0, ν^0, and H^0.

It is also worthwhile to compare the size of formulations (2.6) and (2.7) for a surface of codimension 1 in $\mathbb{R}^n$: without the ODE present in both cases, weak formulation (2.7) is of size $2n + 1$, while the new weak system given in (2.6) is of size $n^2 + n$ (the first equation is merely an identity).

We note that the first equation determining v could be simplified to the natural pointwise identity $v = -H\nu$ (see [30]).

3. Evolving surface finite element semi-discretization

3.1. Evolving surface finite elements

We formulate the evolving surface finite element (ESFEM) discretization for the velocity law coupled with evolution equations on the evolving surface following the description in [28,31], which is based on [17,19,27]. We use simplicial finite elements and continuous piecewise polynomial basis functions of degree k, as defined in [17, Section 2.5].

We triangulate the given smooth initial surface Γ^0 by an admissible family of triangulations $\mathcal{T}_h$ of decreasing maximal element diameter h; see [22] for the notion of an admissible triangulation, which includes quasi-uniformity and shape regularity. For a momentarily fixed h, we denote by $\mathbf{x}^0$ the vector in $\mathbb{R}^{nN}$ that collects all nodes p_j ($j = 1, \dots, N$) of the initial triangulation. By piecewise polynomial interpolation of degree k, the nodal vector defines an approximate surface Γ_h^0 that interpolates Γ^0 in the nodes p_j. We will evolve the jth node in time, denoted by $x_j(t)$ with $x_j(0) = p_j$, and collect the nodes at time t in a column vector

$$\mathbf{x}(t) \in \mathbb{R}^{Nn}.$$

We just write $\mathbf{x}$ for $\mathbf{x}(t)$ when the dependence on t is not important.

By piecewise polynomial interpolation on the plane reference triangle that corresponds to every curved triangle of the triangulation, the nodal vector $\mathbf{x}$ defines a closed surface denoted by $\Gamma_h[\mathbf{x}]$. We can then define globally continuous finite element *basis functions*

$$\phi_i[\mathbf{x}] : \Gamma_h[\mathbf{x}] \to \mathbb{R}, \quad i = 1, \dots, N,$$

which have the property that on every triangle, their pullback to the reference triangle is a polynomial of degree k which satisfies at the nodes $\phi_i[\mathbf{x}](x_j) = \delta_{ij}$ for all $i, j = 1, \dots, N$. These functions span the finite element space on $\Gamma_h[\mathbf{x}]$, that is,

$$S_h[\mathbf{x}] = S_h(\Gamma_h[\mathbf{x}]) = \operatorname{span}\{\phi_1[\mathbf{x}], \phi_2[\mathbf{x}], \dots, \phi_N[\mathbf{x}]\}.$$

For a finite element function $u_h \in S_h[\mathbf{x}]$, the tangential gradient $\nabla_{\Gamma_h[\mathbf{x}]} u_h$ is defined piecewise on each element.

The discrete surface at time t is parametrized by the initial discrete surface via the map $X_h(\cdot, t) : \Gamma_h^0 \to \Gamma_h[\mathbf{x}(t)]$ defined by

$$X_h(p_h, t) = \sum_{j=1}^{N} x_j(t)\, \phi_j[\mathbf{x}(0)](p_h), \quad p_h \in \Gamma_h^0,$$

which has the properties that $X_h(p_j, t) = x_j(t)$ for $j = 1, \dots, N$, $X_h(p_h, 0) = p_h$ for all $p_h \in \Gamma_h^0$, and

$$\Gamma_h[\mathbf{x}(t)] = \Gamma[X_h(\cdot, t)] = \{X_h(p_h, t) \mid p_h \in \Gamma_h^0\}.$$

The *discrete velocity* $v_h(x, t) \in \mathbb{R}^n$ at a point $x = X_h(p_h, t) \in \Gamma[X_h(\cdot, t)]$ is given by

$$\partial_t X_h(p_h, t) = v_h(X_h(p_h, t), t).$$

In view of the transport property of the basis functions [22], $\frac{\mathrm{d}}{\mathrm{d}t}(\phi_j[\mathbf{x}(t)](X_h(p_h, t))) = 0$, the discrete velocity equals, for $x \in \Gamma_h[\mathbf{x}(t)]$,

$$v_h(x, t) = \sum_{j=1}^{N} v_j(t)\, \phi_j[\mathbf{x}(t)](x) \quad \text{with} \quad v_j(t) = \dot{x}_j(t),$$

where the dot denotes the time derivative $\mathrm{d}/\mathrm{d}t$. Hence, the discrete velocity $v_h(\cdot, t)$ is in the finite element space $S_h[\mathbf{x}(t)]$, with nodal vector $\mathbf{v}(t) = \dot{\mathbf{x}}(t)$.

The *discrete material derivative* of a finite element function $u_h(x, t)$ with nodal values $u_j(t)$ is

$$\partial_h^\bullet u_h(x, t) = \frac{\mathrm{d}}{\mathrm{d}t} u_h(X_h(p_h, t)) = \sum_{j=1}^{N} \dot{u}_j(t) \phi_j[\mathbf{x}(t)](x) \quad \text{at} \quad x = X_h(p_h, t).$$

3.2. ESFEM spatial semi-discretizations

Now we describe the semi-discretization of the coupled system for mean curvature flow in arbitrary codimension.

The finite element spatial semi-discretization of the weak coupled parabolic system (see (2.6)) reads as follows: Find the unknown nodal vector $\mathbf{x}(t) \in \mathbb{R}^{Nn}$ and the unknown finite element functions $v_h(\cdot,t) \in S_h[\mathbf{x}(t)]^n$ and $\pi_h(\cdot,t) \in S_h[\mathbf{x}(t)]^{n\times n}$, as well as $\vec{H}_h(\cdot,t) \in S_h[\mathbf{x}(t)]^n$, satisfying the coupled semi-discrete system

$$v_h = \vec{H}_h, \tag{3.1a}$$

$$\int_{\Gamma_h[\mathbf{x}]} \partial_h^\bullet \pi_h \cdot \varphi_h^\pi + \int_{\Gamma_h[\mathbf{x}]} \nabla_{\Gamma_h[\mathbf{x}]}\pi_h \cdot \nabla_{\Gamma_h[\mathbf{x}]}\varphi_h^\pi = \int_{\Gamma_h[\mathbf{x}]} f_1(\pi_h)\cdot\varphi_h^\pi, \tag{3.1b}$$

$$\int_{\Gamma_h[\mathbf{x}]} \partial_h^\bullet \vec{H}_h \cdot \varphi_h^{\vec{H}} + \int_{\Gamma_h[\mathbf{x}]} \nabla_{\Gamma_h[\mathbf{x}]}\vec{H}_h \cdot \nabla_{\Gamma_h[\mathbf{x}]}\varphi_h^{\vec{H}} = \int_{\Gamma_h[\mathbf{x}]} f_2(\pi_h,\vec{H}_h)\cdot\varphi_h^{\vec{H}}, \tag{3.1c}$$

where $f_1(\pi_h)$ and $f_2(\pi_h,\vec{H}_h)$ are the spatially discrete analogues of non-linear expressions (2.4), for all $\varphi_h^\pi \in S_h[\mathbf{x}(t)]^{n\times n}$ and $\varphi_h^{\vec{H}} \in S_h[\mathbf{x}(t)]^n$, with the surface $\Gamma_h[\mathbf{x}(t)] = \Gamma[X_h(\cdot,t)]$ given by the differential equation

$$\partial_t X_h(p_h,t) = v_h(X_h(p_h,t),t), \quad p_h \in \Gamma_h^0. \tag{3.2}$$

The initial values for the nodal vector $\mathbf{x}$ are taken as the positions of the nodes of the triangulation of the given initial surface Γ^0. The initial data π_h^0 and $\vec{H}_h^0$ are determined by componentwise Lagrange interpolation of π^0 and $\vec{H}^0$.

3.3. Matrix–vector formulation

The nodal values of the unknown semi-discrete functions $v_h(\cdot,t) \in S_h[\mathbf{x}(t)]^n$, $\pi_h(\cdot,t) \in S_h[\mathbf{x}(t)]^{n\times n}$, and $\vec{H}(\cdot,t) \in S_h[\mathbf{x}(t)]^n$ are collected into column vectors $\mathbf{v}(t) = (v_j(t)) \in \mathbb{R}^{Nn}$, $\boldsymbol{\pi}(t) = (\pi_j(t)) \in \mathbb{R}^{Nn^2}$, and $\vec{\mathbf{H}}(t) = (\vec{H}_j(t)) \in \mathbb{R}^{Nn}$, respectively. Furthermore, we set

$$\mathbf{u} = \begin{pmatrix} \boldsymbol{\pi} \\ \vec{\mathbf{H}} \end{pmatrix} \in \mathbb{R}^{N(n^2+n)}$$

and set $\boldsymbol{I}$ to be a block matrix extracting the $\vec{\mathbf{H}}$ component of $\mathbf{u}$, that is, $\boldsymbol{I}\mathbf{u} = \vec{\mathbf{H}}$.

We define the surface-dependent mass matrix $\mathbf{M}(\mathbf{x})$ and stiffness matrix $\mathbf{A}(\mathbf{x})$ by

$$\mathbf{M}(\mathbf{x})|_{ij} = \int_{\Gamma_h[\mathbf{x}]} \phi_i[\mathbf{x}]\phi_j[\mathbf{x}] \quad \text{and} \quad \mathbf{A}(\mathbf{x})|_{ij} = \int_{\Gamma_h[\mathbf{x}]} \nabla_{\Gamma_h[\mathbf{x}]}\phi_i[\mathbf{x}] \cdot \nabla_{\Gamma_h[\mathbf{x}]}\phi_j[\mathbf{x}],$$

for $i, j = 1,\dots,N$. The non-linear terms $\mathbf{f}(\mathbf{x},\mathbf{u}) = (\mathbf{f}_1(\mathbf{x},\mathbf{u}),\mathbf{f}_2(\mathbf{x},\mathbf{u}))^T$ are defined by

$$\mathbf{f}_1(\mathbf{x},\mathbf{u})|_{k+(\alpha-1)N+(\beta-1)nN} = \int_{\Gamma_h[\mathbf{x}]} f_1(\pi_h)_{\alpha\beta}\ \phi_k[\mathbf{x}],$$

$$\mathbf{f}_2(\mathbf{x},\mathbf{u})|_{k+(\alpha-1)N} = \int_{\Gamma_h[\mathbf{x}]} f_2(\pi_h, \vec{H}_h)_\alpha \, \phi_k[\mathbf{x}]$$

for $k = 1,\dots,N$ and $\alpha,\beta = 1,\dots,n$.

Furthermore, for $d \in \mathbb{N}$ (with the identity matrices $I_d \in \mathbb{R}^{d\times d}$), we let

$$\mathbf{M}^{[d]}(\mathbf{x}) = I_d \otimes \mathbf{M}(\mathbf{x}), \quad \mathbf{A}^{[d]}(\mathbf{x}) = I_d \otimes \mathbf{A}(\mathbf{x}).$$

When no confusion can arise, we will write $\mathbf{M}(\mathbf{x})$ for $\mathbf{M}^{[d]}(\mathbf{x})$ and $\mathbf{A}(\mathbf{x})$ for $\mathbf{A}^{[d]}(\mathbf{x})$.

Using the definitions given in (3.1), (3.2) can be written in the matrix–vector form

$$\begin{aligned} \mathbf{v} &= \boldsymbol{I}\,\mathbf{u}, \\ \mathbf{M}(\mathbf{x})\dot{\mathbf{u}} + \mathbf{A}(\mathbf{x})\mathbf{u} &= \mathbf{f}(\mathbf{x},\mathbf{u}), \\ \text{with} \qquad \dot{\mathbf{x}} &= \mathbf{v}. \end{aligned} \tag{3.3}$$

Matrix–vector formulation (3.3) for mean curvature flow in arbitrary codimension is almost identical to the same formulas for mean curvature flow in codimension 1 (see [28, (3.4)–(3.5)]):

$$\begin{aligned} (\mathbf{M}(\mathbf{x}) + \mathbf{A}(\mathbf{x}))\mathbf{v} &= \mathbf{g}(\mathbf{x},\mathbf{u}), \\ \mathbf{M}(\mathbf{x})\dot{\mathbf{u}} + \mathbf{A}(\mathbf{x})\mathbf{u} &= \mathbf{f}(\mathbf{x},\mathbf{u}), \\ \text{with} \quad \dot{\mathbf{x}} &= \mathbf{v}. \end{aligned}$$

In the two above ODE systems, the equations for $\mathbf{u}$ and $\mathbf{x}$ are formally the same, though the equation for $\mathbf{v}$ is even simpler here. Note that here $\mathbf{u}$ collects $\boldsymbol{\pi}$ and $\vec{\mathbf{H}}$, whereas for mean curvature flow in codimension 1 it collects $\mathbf{u} = (\mathbf{n}, \mathbf{H})^T$, that is, the nodal values of the approximations to the normal vector and scalar mean curvature. Naturally, the block-size of the matrices in the two equations for $\mathbf{u}$ are different ($n^2 + n$ and $n + 1$, respectively).

It is crucial to notice that, thanks to the coinciding matrix–vector formulations, many results from [28]—most notably, the stability results given by Propositions 7.1 and 10.1 therein—hold directly for the present case as well.

3.4. Lifts

As in [31] and [28, Section 3.4], we compare functions on the *exact surface* $\Gamma[X(\cdot,t)]$ with functions on the *discrete surface* $\Gamma_h[\mathbf{x}(t)]$ via functions on the *interpolated surface* $\Gamma_h[\mathbf{x}^*(t)]$, where $\mathbf{x}^*(t)$ denotes the nodal vector collecting the grid points $x_j^*(t) = X(p_j,t)$ on the exact surface, and p_j are the nodes of the discrete initial triangulation Γ_h^0.

Any finite element function w_h on the discrete surface, with nodal values w_j, is associated with a finite element function $\widehat{w}_h$ on the interpolated surface $\Gamma_h[\mathbf{x}^*]$ with the exact same nodal values. This can be further lifted to a function on the exact surface by using the *lift operator* $^\ell$, mapping a function on the interpolated surface $\Gamma_h[\mathbf{x}^*]$ to a function on

the exact surface $\Gamma[X]$, via the *closest point projection*. Provided that the two surfaces are sufficiently close, for $x \in \Gamma_h[\mathbf{x}^*]$, find $x^\ell \in \Gamma[X]$ such that $x^\ell - x$ is minimal, that is,

$$x^\ell - x \perp T_{x^\ell}\Gamma[X], \quad \text{and then set} \quad \widehat{w}_h^\ell(x^\ell) = \widehat{w}_h(x).$$

This definition is consistent with the lift operator in codimension 1 (see [17, 19, 22]) using the signed distance function d. The standard norm-equivalence results given by [17, (2.15)–(2.17)] hold for this definition as well.

Then, the composed lift ^{L} maps finite element functions on the discrete surface $\Gamma_h[\mathbf{x}]$ to functions on the exact surface $\Gamma[X]$ via the interpolated surface $\Gamma_h[\mathbf{x}^*]$, and it is defined by

$$w_h^L = (\widehat{w}_h)^\ell.$$

4. Linearly implicit full discretization

Similar to the case of mean curvature flow [28], for the time discretization of system of ordinary differential equations (3.3), we use a q-step linearly implicit backward difference formula (BDF method). For a step size $\tau > 0$, and with $t_n = n\tau \le T$, we determine the approximations to all variables $\mathbf{x}^n$ to $\mathbf{x}(t_n)$, $\mathbf{v}^n$ to $\mathbf{v}(t_n)$, and $\mathbf{u}^n$ to $\mathbf{u}(t_n)$ by the fully discrete system of *linear* equations

$$\mathbf{v}^n = \boldsymbol{I}\,\mathbf{u}^n, \tag{4.1a}$$

$$\mathbf{M}(\widetilde{\mathbf{x}}^n)\dot{\mathbf{u}}^n + \mathbf{A}(\widetilde{\mathbf{x}}^n)\mathbf{u}^n = \mathbf{f}(\widetilde{\mathbf{x}}^n, \widetilde{\mathbf{u}}^n), \tag{4.1b}$$

$$\dot{\mathbf{x}}^n = \mathbf{v}^n, \tag{4.1c}$$

where we denote the discretized time derivatives

$$\dot{\mathbf{x}}^n = \frac{1}{\tau}\sum_{j=0}^{q} \delta_j \mathbf{x}^{n-j}, \quad \dot{\mathbf{u}}^n = \frac{1}{\tau}\sum_{j=0}^{q} \delta_j \mathbf{u}^{n-j}, \qquad n \ge q,$$

and where $\widetilde{\mathbf{x}}^n$ and $\widetilde{\mathbf{u}}^n$ are the extrapolated values

$$\widetilde{\mathbf{x}}^n = \sum_{j=0}^{q-1} \gamma_j \mathbf{x}^{n-1-j}, \quad \widetilde{\mathbf{u}}^n = \sum_{j=0}^{q-1} \gamma_j \mathbf{u}^{n-1-j}, \qquad n \ge q. \tag{4.2}$$

The starting values $\mathbf{x}^i$ and $\mathbf{u}^i$ $(i = 0, \dots, q-1)$ are assumed to be given; in addition, we set $\widetilde{\mathbf{x}}^i = \mathbf{x}^i$ and $\widetilde{\mathbf{u}}^i = \mathbf{u}^i$ for $i = 0, \dots, q-1$. They can be precomputed using either a lower-order method with smaller step sizes or an implicit Runge–Kutta method.

The method is determined by its coefficients, which are given by $\delta(\zeta) = \sum_{j=0}^{q} \delta_j \zeta^j = \sum_{\ell=1}^{q} \frac{1}{\ell}(1-\zeta)^\ell$ and $\gamma(\zeta) = \sum_{j=0}^{q-1} \gamma_j \zeta^j = (1-(1-\zeta)^q)/\zeta$. The classical BDF method

is known to be zero-stable for $q \leq 6$ and to have order q; see [25, Chapter V]. This order is retained, for $q \leq 5$, by the linearly implicit variant using the above-mentioned coefficients γ_j (cf. [2,33]).

We again point out that fully discrete system (4.1)–(4.3) is formally the same as the fully discrete system for the mean curvature flow for surfaces [28, (5.1)–(5.4)]. In [28, Theorem 6.1] optimal-order error bounds for the combined ESFEM–BDF full discretization of the mean curvature flow system are proved, for finite elements of polynomial degree $k \geq 2$ and BDF methods of order $2 \leq q \leq 5$.

We note that in the nth time step, the method decouples and hence only requires solving a linear system with the symmetric positive definite matrix $\delta_0 \mathbf{M}(\widetilde{\mathbf{x}}^n) + \tau \mathbf{A}(\widetilde{\mathbf{x}}^n)$.

From the vectors and matrices $\mathbf{x}^n = (x_j^n)$, $\mathbf{v}^n = (v_j^n)$, and $\mathbf{u}^n = (u_j^n)$ with $u_j^n = (\pi_j^n, \vec{H}_j^n)$, where $\pi_j^n \in \mathbb{R}^{n\times n}$ and $\vec{H}_j^n \in \mathbb{R}^n$, we obtain position approximations to $X(\cdot, t_n)$ and $\mathrm{id}_{\Gamma[X(\cdot,t_n)]}$, velocity approximations to $v(\cdot, t_n)$, and approximations to the orthogonal projection and the mean curvature vector, respectively, at time t_n as

$$\begin{aligned}
X_h^n(p_h) &= \sum_{j=1}^N x_j^n \, \phi_j[\mathbf{x}(0)](p_h) && \text{for } p_h \in \Gamma_h^0,\\
x_h^n(x) &= \mathrm{id}_{\Gamma[X_h^n]},\\
v_h^n(x) &= \sum_{j=1}^N v_j^n \, \phi_j[\mathbf{x}^n](x) && \text{for } x \in \Gamma_h[\mathbf{x}^n],\\
\pi_h^n(x) &= \sum_{j=1}^N \pi_j^n \, \phi_j[\mathbf{x}^n](x) && \text{for } x \in \Gamma_h[\mathbf{x}^n],\\
\vec{H}_h^n(x) &= \sum_{j=1}^N \vec{H}_j^n \, \phi_j[\mathbf{x}^n](x) && \text{for } x \in \Gamma_h[\mathbf{x}^n].
\end{aligned} \tag{4.3}$$

In the semi-discrete case, the approximations of the same quantities are given analogously.

5. Main results: Error estimates

We are now in the position to state the main results of this paper—namely, time-uniform optimal-order semi- and fully discrete H^1-norm error estimates for the position, velocity, orthogonal projection, and mean curvature vector obtained, respectively, by semi-discretization (3.1) (or (3.3)), or linearly implicit BDF full discretization (4.1), using evolving surface finite elements of polynomial degree at least 2, and q-step BDF method with $2 \leq q \leq 5$.

5.1. Convergence of the semi-discretization

Theorem 5.1. *Consider semi-discretization (3.1) of the mean curvature flow in (2.2) in arbitrary codimension $n-m$, using evolving surface finite elements of polynomial degree $k \geq 2$. Suppose that the mean curvature flow problem in arbitrary codimension admits an exact solution $(X, v, \pi, \vec{H})$ that is sufficiently smooth on the time interval $t \in [0, T]$, and that the flow map $X(\cdot, t) : \Gamma^0 \to \Gamma(t) \subset \mathbb{R}^n$ is non-degenerate so that $\Gamma(t) = \Gamma[X(\cdot, t)]$ is a regular surface on the time interval $t \in [0, T]$.*

Then, there exist constants $h_0 > 0$ and $C > 0$ such that

$$\begin{aligned}
\|x_h^L(\cdot, t) - \mathrm{id}_{\Gamma(t)}\|_{H^1(\Gamma(t))} &\leq C h^k, \\
\|v_h^L(\cdot, t) - v(\cdot, t)\|_{H^1(\Gamma(t))} &\leq C h^k, \\
\|\pi_h^L(\cdot, t) - \pi(\cdot, t)\|_{H^1(\Gamma(t))} &\leq C h^k, \\
\|\vec{H}_h^L(\cdot, t) - \vec{H}(\cdot, t)\|_{H^1(\Gamma(t))} &\leq C h^k, \\
\|X_h^\ell(\cdot, t) - X(\cdot, t)\|_{H^1(\Gamma^0)} &\leq C h^k,
\end{aligned}$$

for all $h \leq h_0$. The constant $C > 0$ is independent of h and t, but depends on the H^{k+1}-norms of the exact solution $(X, v, \pi, \vec{H})$ and on the final time T.

Proof. The result essentially follows from the proof of [28, Theorem 4.1].

The stability is shown following the proof of [28, Proposition 7.1], since (as we have pointed out above) matrix–vector formulation (3.3) is (almost) identical to the matrix–vector formulation of [28, (3.4)–(3.5)] (recalling that here $\mathbf{u} = (\boldsymbol{\pi}, \vec{\mathbf{H}})^T$ is in the role of $\mathbf{u} = (\mathbf{n}, \mathbf{H})^T$ in [28]). The system uses the same mass and stiffness matrices (but of different size), while the proof therein only uses the local Lipschitz continuity of the nonlinear terms, which holds here as well. The bounded operator $\boldsymbol{I}$ in the velocity equation $\mathbf{v} = \boldsymbol{I}\mathbf{u}$ even simplifies part (B) of the stability proof of [28, Proposition 7.1].

The consistency errors for $(X, v, \pi, \vec{H})$ are shown by the exact techniques of the consistency analysis [28, Lemma 8.1].

The uniform-in-time H^1-norm error bounds are proved by combining stability and consistency, verbatim as in [28, Section 9]. ∎

5.2. Convergence of the full discretization

Theorem 5.2. *Consider full discretization (4.1) of the mean curvature flow in (2.2) in arbitrary codimension $n-m$, using evolving surface finite elements of polynomial degree $k \geq 2$ and linearly implicit BDF time discretization of order q with $2 \leq q \leq 5$. Suppose that the mean curvature flow problem in arbitrary codimension admits an exact solution $(X, v, \pi, \vec{H})$ that is sufficiently smooth on the time interval $t \in [0, T]$, and that the flow map $X(\cdot, t) : \Gamma^0 \to \Gamma(t) \subset \mathbb{R}^n$ is non-degenerate so that $\Gamma(t) = \Gamma[X(\cdot, t)]$ is a regular surface on the time interval $t \in [0, T]$.*

Then, there exist constants $h_0 > 0$, $\tau_0 > 0$, and $C_0 > 0$ such that for all mesh sizes $h \le h_0$ and time step sizes $\tau \le \tau_0$ satisfying the mild step size restriction

$$\tau \le C_0 h$$

(where $C_0 > 0$ can be chosen arbitrarily), the following error bounds for the lifts of the discrete position, velocity, tangential projection and mean curvature vector hold over the exact surface: provided that the starting values are $\mathcal{O}(h^k + \tau^{q+1/2})$ accurate in the H^1 norm at time t_i for $i = 0, \dots, q-1$, we have at time $t_n = n\tau \le T$

$$\begin{aligned}
\|(x_h^n)^L - \mathrm{id}_{\Gamma(t_n)}\|_{H^1(\Gamma(t_n))} &\le C(h^k + \tau^q),\\
\|(v_h^n)^L - v(\cdot, t_n)\|_{H^1(\Gamma(t_n))} &\le C(h^k + \tau^q),\\
\|(\pi_h^n)^L - \pi(\cdot, t_n)\|_{H^1(\Gamma(t_n))} &\le C(h^k + \tau^q),\\
\|(\vec{H}_h^n)^L - \vec{H}(\cdot, t_n)\|_{H^1(\Gamma(t_n))} &\le C(h^k + \tau^q),\\
\|(X_h^n)^\ell - X(\cdot, t_n)\|_{H^1(\Gamma^0)} &\le C(h^k + \tau^q)
\end{aligned}$$

for all $h \le h_0$. The constant $C > 0$ is independent of h, τ, and n, but depends on bounds of higher derivatives of the exact solution $(X, v, \pi, \vec{H})$, on the final time T, and on C_0.

Proof. The proof is similar to the case of semi-discrete error bounds: since the ESFEM/linearly implicit BDF discretization given in (4.1) is (almost) identical to [28, (5.1)], the proof of this result directly follows as the proof of [28, Theorem 6.1]. ∎

For *surfaces* in *codimension at least two*, Theorems 5.1 and 5.2 provide (to our knowledge) the first convergence results. However, for *curves* in higher codimension, simpler methods with convergence analysis are available; see [15,21,37].

For *surfaces* in *codimension 1*, although Theorems 5.1 and 5.2 hold, we recommend the use of the convergent methods of [28] (which requires polynomial degree $k \ge 2$) or Dziuk [20, 32] (which requires polynomial degree $k \ge 6$). We note that other attractive methods—without a convergence analysis—are available; for these, see the references in [28].

Remark 5.3. The stability and convergence results readily extend to higher-dimensional submanifolds $\Gamma[X] \subset \mathbb{R}^n$ of dimension $m \ge 4$ and of arbitrary codimension $n - m$ (cf. [28, Section 14]), provided that a suitable optimal-order (quasi-)interpolation is used to counter the effect of the inverse estimates instead of the nodal interpolation (cf. [23, Lemma 4.3], which requires dimension $m \le 3$), and requires evolving surface finite elements of degree $k \ge \lfloor m/2 \rfloor + 1$ and BDF methods of order $\lfloor m/2 \rfloor + 1 \le q \le 5$. For the six-step BDF method, a new multiplier-based energy technique was developed in [1]. The fully discrete stability proof in [28] should generalize to this approach.

6. Numerical examples for curves in $\mathbb{R}^3$

We performed the following numerical experiments for mean curvature flow of curves in $\mathbb{R}^3$:

- A convergence test using planar curves where the exact solution is known.
- A comparison test with Dziuk's algorithm for curves [16] using circles and Angenent ovals [8].
- Experiments for space curves using established examples from the literature [10, 37] (e.g., a trefoil knot), still comparing with Dziuk's algorithm.

All our numerical experiments were carried out in Matlab using quadratic evolving surface finite elements and BDF methods of various order specified in the experiments. The parametrization of the quadratic elements was inspired by [12]. The initial meshes were all generated using an arc-length parametrization, without taking advantage of any symmetry of the surface.

6.1. Convergence test

We are reporting on the errors of our algorithm for mean curvature flow in codimension 2 for *flat space curves*. Simple test examples are constructed in this setting by using the fact that the evolution of flat space curves evolving under the flow given by (2.2) is equivalent to their evolution under *curve shortening flow*.

Let the curve $\Gamma^0 : [0, 2\pi] \to \mathbb{R}^3$ be a circle of initial radius R_0 in an arbitrary plane.

We consider the mean curvature flow of $\Gamma(\cdot, t)$ with initial value Γ_0. Using the rotational symmetry of Γ along flow, we obtain that its radius satisfies the ODE

$$\frac{\mathrm{d}}{\mathrm{d}t} R(t) = -\frac{1}{R(t)} \quad \text{with initial value} \quad R(0) = R_0.$$

The above initial value problem has the solution

$$R(t) = \sqrt{R_0^2 - 2t}$$

until final time $T_{\max} = R_0^2/2$. Therefore, the curvature of $\Gamma(\cdot, t)$ is given by the formula $H(\cdot, t) = 1/R(t) = (R_0^2 - 2t)^{-1/2}$.

We computed numerical approximations to the flow using quadratic finite elements ($k = 2$) and using the 2-step linearly implicit BDF method ($q = 2$) for a circle of radius $R_0 = 1$ which lies in the y–z-plane rotated by $\theta = \pi/e$. The starting values $\mathbf{x}^i \in \mathbb{R}^{3N}$ and $\mathbf{u} = (\boldsymbol{\pi}, \mathbf{H})^T \in \mathbb{R}^{(9+3)N}$ for $i = 1, \ldots, q-1$ were computed as the interpolations of the exact values.

In Figures 1 and 2 we report on the errors between the numerical and (interpolation of) exact solutions for mean curvature flow in codimension 2 of a flat circle until the final time $T_{\max}$, illustrating the error bounds of Theorems 5.1 and 5.2. The two plots in Figure 1

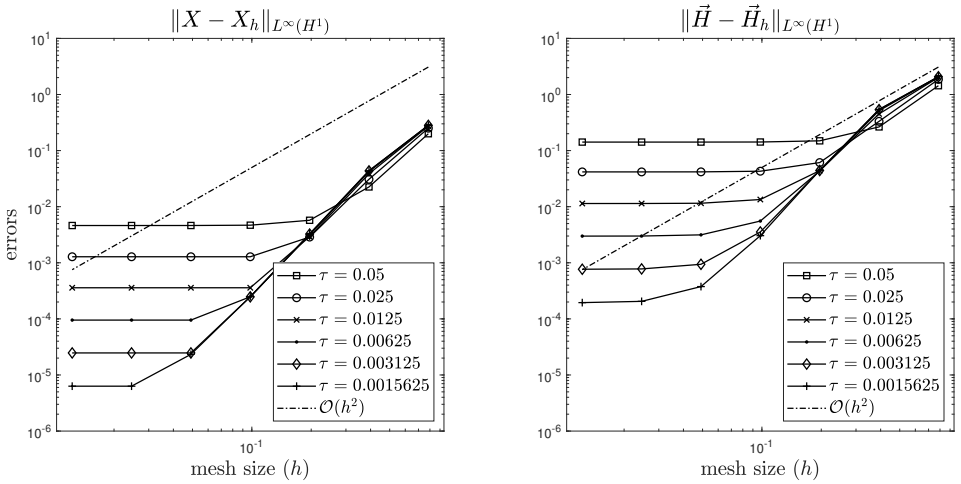

Figure 1. Spatial convergence of the BDF2/ quadratic ESFEM discretization for MCF codimension 2 of the unit circle for $T = 0.4$.

report on the surface error and the errors of the mean curvature $\vec{H}_h$ on the left- and right-hand side, respectively. The logarithmic error plots show the $L^\infty(H^1)$-norm errors against the mesh size h. The lines marked with different symbols correspond to different time step sizes τ. Figure 2 reports on the same errors but reversing roles of h and τ.

In both cases the error curves match the slope of the reference lines (dashed) corresponding to the convergence order of Theorems 5.1 and 5.2, $\mathcal{O}(h^2)$ and $\mathcal{O}(\tau^2)$.

6.2. Comparison with Dziuk's algorithm

We compared algorithm (4.1) with (the linearly implicit BDF version of) Dziuk's algorithm for curves; see [16, 21]:

$$\mathbf{M}(\widetilde{\mathbf{x}}^n)\dot{\mathbf{x}}^n + \mathbf{A}(\widetilde{\mathbf{x}}^n)\mathbf{x}^n = 0 \quad \text{for } n \geq q, \tag{6.1}$$

with given initial data $\mathbf{x}^i \in \mathbb{R}^{3N}$ for $i = 1, \ldots, q-1$. Naturally, Dziuk's algorithm is considerably faster in each time step. Comparing (4.1) and (6.1), for the former we additionally need to assemble the non-linear term $\mathbf{f}$; moreover, for curves in n, the linear equation systems have block sizes $n^2 + n$ and n, respectively (each of size N for a mesh with N nodes). Further numerical comparisons are not reported here.

Figure 3 compares the exact solution (black), Dziuk's algorithm (gray), and our algorithm (4.1) (light gray) for a flat circle of unit radius over the time interval $[0, 0.4875]$, using a mesh with 128 nodes and $\tau = 0.0125$.

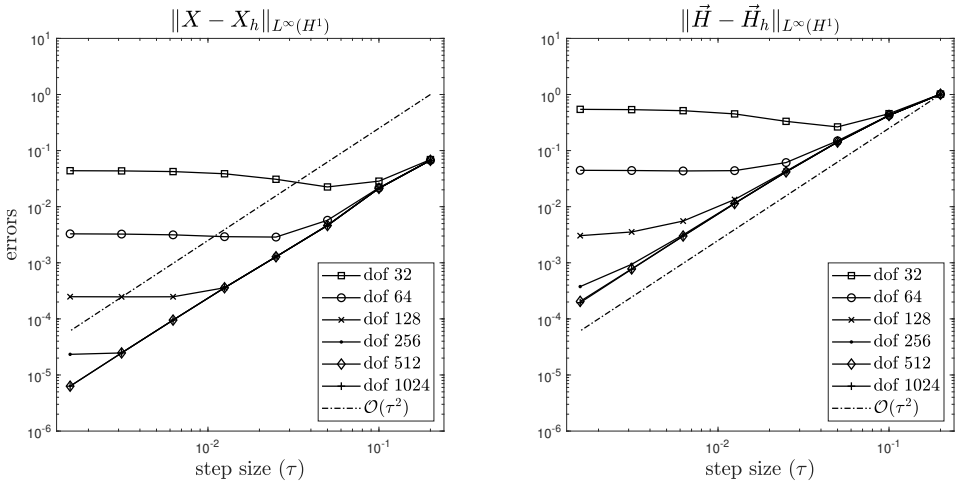

Figure 2. Temporal convergence of the BDF2/ quadratic ESFEM discretization for MCF codimension 2 of the unit circle for $T = 0.4$.

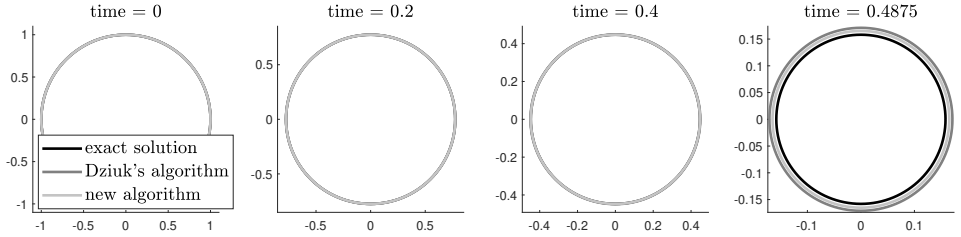

Figure 3. Comparing our algorithm (light gray) with the exact solution (black) and Dziuk's algorithm (gray) using a flat circle.

Figure 4 reports on the same comparison for another family of known (ancient) solutions Angenent ovals defined, for $\theta \in [0, 2\pi]$ and $t \in (-\infty, 0)$, by

$$X(\theta, t) = \Big(\int_0^r \cos(\varphi)\kappa(\varphi)^{-1} \mathrm{d}\varphi,\ \int_0^r \cos(\varphi)\kappa(\varphi)^{-1} \mathrm{d}\varphi,\ 0 \Big), \quad \text{with} \quad \kappa^2(\varphi, t) = (e^{-2t} - 1)^{-1} + \cos^2(\varphi); \tag{6.2}$$

for more details, we refer to [8]. Choosing Γ^0 as the Angenent oval with $t_0 < 0$ via (6.2), a solution exists on the interval $[0, -t_0)$.

The comparison experiment of Figure 4 was performed on the time interval $[0, 2]$ using the Angenent oval with $t_0 = -2$ as initial values Γ^0, using a mesh with 128 nodes and $\tau = 10^{-4}$. In the figure the numerical solutions overlap the exact solution (in black).

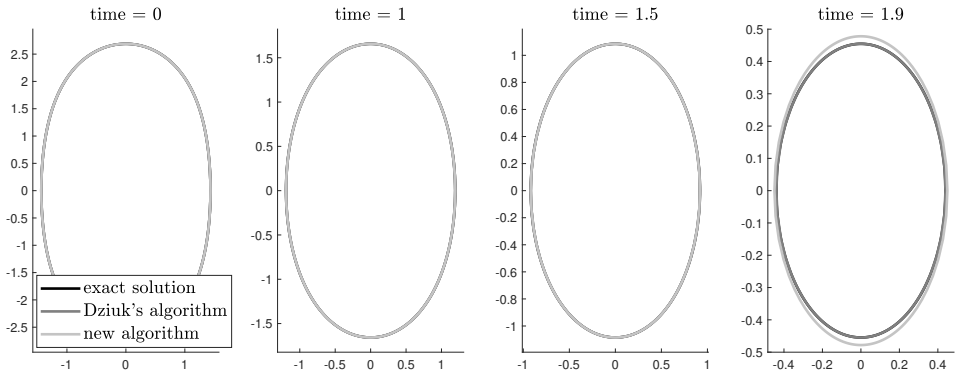

Figure 4. Comparing our algorithm (light gray) with the exact solution (black) and Dziuk's algorithm (gray) using (flat) Angenent ovals (see (6.2)).

6.3. Experiments for space curves

We have performed various experiments for space curves as well, comparing our algorithm and Dziuk's. In Figures 5–7 we report on the time evolution of a sinusoidal curve and a trefoil knot (which is eventually only immersed).

The numerical experiments in [13,28,30] have indicated that it is beneficial to conserve the geometric properties of the dynamic variables close to singularities; for example, for mean curvature flow projecting the extrapolated normal vector back to the unit sphere (cf. (4.2)).

According to our experiments the symmetry of π_h is well preserved; however, the idempotency $\pi_h^2 = \pi_h$ is deteriorating. Figure 5 reports on an experiment where a (regularized) minimization problem is solved (using Matlab's `fmincon`) in order to preserve idempotency, comparing it to the original algorithm. The regularization step is performed only for those extrapolated projection matrices $\widetilde{\pi}_h^n$ (see (4.2)) which are at least a tolerance away from being idempotent. That is a correction step, which is still locally Lipschitz, and is only performed on the right-hand side of (4.1). (Finding an idempotent matrix close to $\widetilde{\pi}_h^n$ is a much harder problem than preserving unit length (cf. [28]). Therefore, this rudimentary process only yields a slight improvement.) In order to highlight this phenomenon, we used a coarse grid (dof $= 64$) and large step size $\tau = 0.01$ for Figure 5. On this very coarse mesh, this loss of idempotency is severe (see the top row of Figure 5), and hence, parts of the solution were cut off during plotting. In the bottom row of Figure 5 we employ the correction step from above using the same mesh. Such a geometric process is used for Figures 6 and 7 as well.

For the evolution of the sinusoidal curve (see Figure 7), we would like to highlight the short time scale and the rapid shrinking along the z-axis.

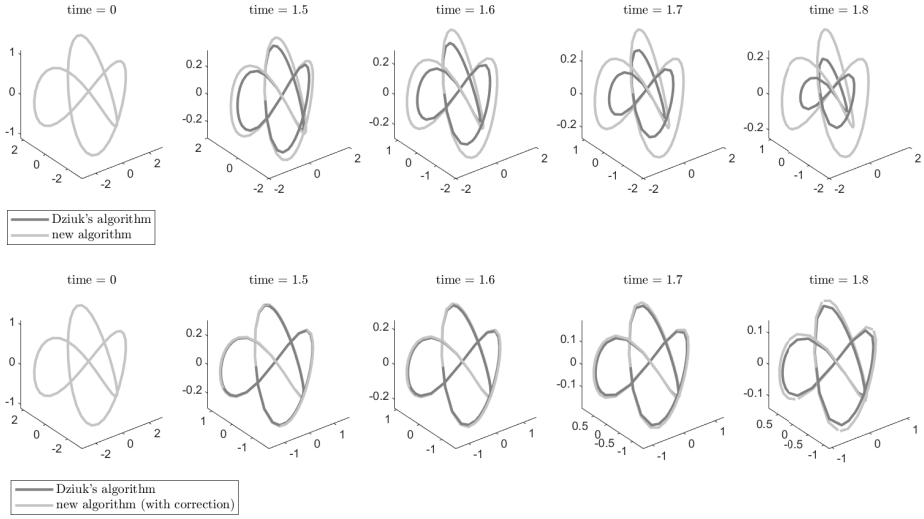

Figure 5. Comparing our algorithm (light gray) without and with idempotency correction (top and bottom), with Dziuk's algorithm (gray) using a trefoil knot as initial value (dof $= 64$ and $\tau = 0.01$).

6.4. Experiments for two-dimensional surfaces of codimension 1

We have also performed experiments for two-dimensional surfaces in $\mathbb{R}^3$ (i.e., in codimension 1), comparing our algorithm (without the projection step for $\widetilde{\pi}_h^n$) with Dziuk's algorithm [20] and with the provably convergent method from [28].

Figure 8 reports on the time evolution of a (rotationally symmetric) dumbbell-shaped initial surface from [24, (2.3)]. We use a time step size $\tau = 10^{-3}$ and mesh with 10522 degrees of freedom.

We emphasize here that this comparison experiment *only* demonstrates that this algorithm indeed works for *codimension 1* surfaces, as stated in Theorems 5.1–5.2 and the introduction. We do not suggest to use this method in the codimension 1 case over either (parametric) algorithms in [9, 20, 28]. The last row of Figure 8 shows a pinch singularity occurring prematurely, due to π_h strongly losing its idempotency. For the sake of completeness, the CPU times for each algorithm are also included.

A. Evolution equations for mean curvature flow in higher codimension

Let $X : \Gamma^0 \times [0, T] \to \mathbb{R}^n$ be a solution of the mean curvature flow, that is,

$$v = \vec{H}.$$

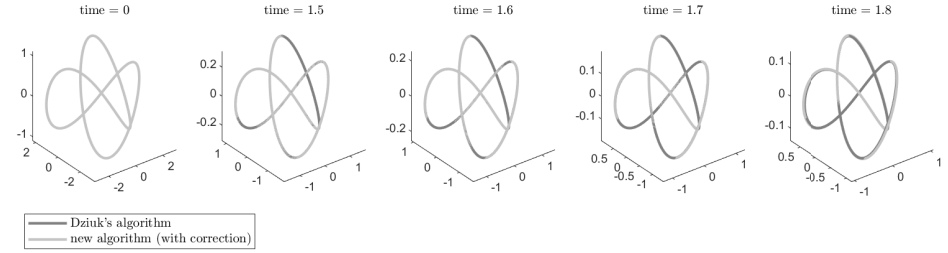

Figure 6. Comparing our algorithm (light gray) with Dziuk's algorithm (gray) using a trefoil knot as initial value (dof $= 512$ and $\tau = 10^{-4}$).

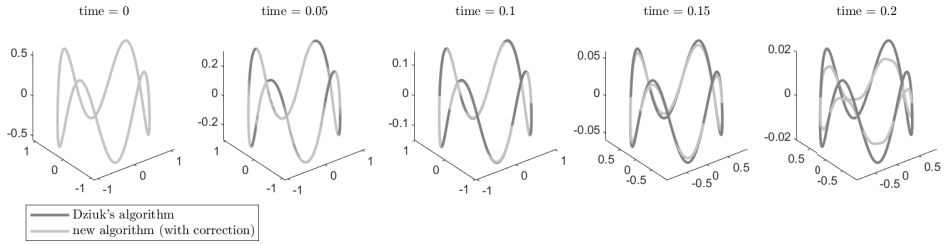

Figure 7. Comparing our algorithm (light gray) with Dziuk's algorithm (gray) using a sinusoidal initial curve (dof $= 512$ and $\tau = 10^{-4}$).

Let $g_{ij} = \partial_i X \cdot \partial_j X = \sum_\mu \partial_i X_\mu \partial_j X_\mu$ denote the induced metric and g^{ij} denote its inverse. Let

$$A_{ij} = (\partial_i \partial_j X)^\perp = \partial_i \partial_j X - \Gamma_{ij}^k \partial_k X$$

denote the second fundamental form and

$$\vec{H} = g^{ij} A_{ij} = (g^{ij} \partial_i \partial_j X)^\perp = g^{ij} \partial_i \partial_j X - g^{ij} \Gamma_{ij}^k \partial_k X$$

the mean curvature vector. We shall view $\vec{H}$ as a function taking values in $\mathbb{R}^n$. Furthermore, let

$$\pi = g^{ij} \partial_i X \otimes \partial_j X$$

be the orthogonal projection from $\mathbb{R}^n$ to the tangent space to the submanifold at the point $X(x,t)$. It can be seen as a function taking values in the space of $n \times n$ matrices.

Lemma A.1. *The evolution of the metric is given by*

$$\frac{\partial}{\partial t} g_{ij} = -2\, \vec{H} \cdot A_{ij}.$$

Moreover, the inverse metric satisfies

$$\frac{\partial}{\partial t} g^{ij} = 2\, g^{ik}\, g^{jl}\, \vec{H} \cdot A_{kl}.$$

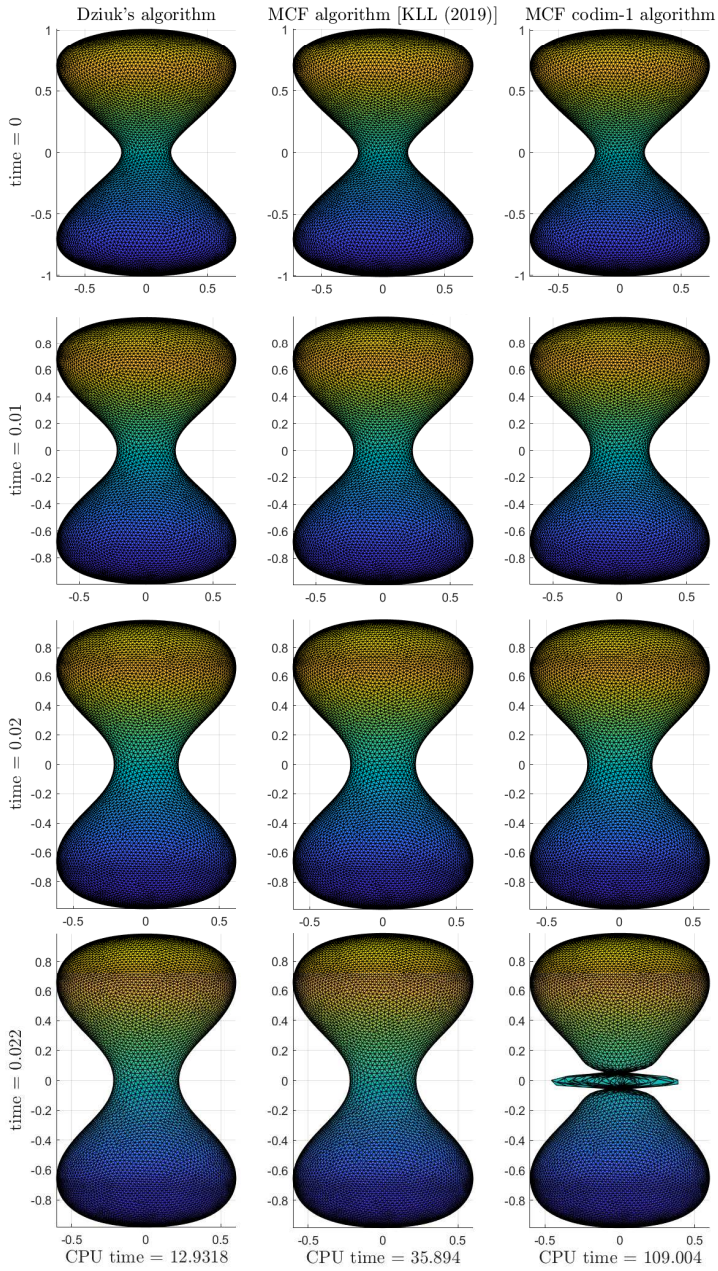

Figure 8. Comparing our algorithm (without projection for $\widetilde{\pi}_h^n$, 3rd column) with Dziuk's algorithm (1st column) and the algorithm of [28] (2nd column) at different times (rows) (dof $= 10522$ and $\tau = 10^{-3}$).

Proof. We compute

$$\frac{\partial}{\partial t} g_{ij} = \partial_i \vec{H} \cdot \partial_j X + \partial_i X \cdot \partial_j \vec{H} = -\vec{H} \cdot \partial_i \partial_j X - \partial_j \partial_i X \cdot \vec{H} = -2\, \vec{H} \cdot A_{ij}.$$

This proves the first statement. Since

$$\frac{\partial}{\partial t} g^{ij} = -g^{ik}\, g^{jl}\, \frac{\partial}{\partial t} g_{kl},$$

the second statement follows. ∎

Lemma A.2. *We have*

$$\frac{\partial}{\partial t} \pi = g^{ij}\, \partial_i \vec{H} \otimes \partial_j X + g^{ij}\, \partial_i X \otimes \partial_j \vec{H} + 2\, g^{ik}\, g^{jl}\, (\vec{H} \cdot A_{kl})\, \partial_i X \otimes \partial_j X.$$

Proof. This follows from the definition of π together with the evolution equation of the metric. ∎

Lemma A.3. *The componentwise derivatives of π are given by*

$$\partial_k \pi = g^{ij}\, A_{ik} \otimes \partial_j X + g^{ij}\, \partial_i X \otimes A_{jk}.$$

Proof. This follows from a direct calculation in geodesic normal coordinates. ∎

In the following, Latin indices will run from 1 to m, and Greek indices will run from 1 to n:

Lemma A.4. *The componentwise Laplacian of π, that is, the Laplacian of π such that $(\Delta\pi)_{\alpha\beta} = \Delta\pi_{\alpha\beta}$, where the Laplacian on the right-hand side is the Laplace–Beltrami operator of the scalar-valued function $\pi_{\alpha\beta}$, is given by*

$$\begin{aligned}\Delta\pi = {} & g^{ij}\, \partial_i \vec{H} \otimes \partial_j X + g^{ij}\, \partial_i X \otimes \partial_j \vec{H} + 2\, g^{ip}\, g^{jq}\, (\vec{H} \cdot A_{ij})\, \partial_p X \otimes \partial_q X \\ & - 2\, g^{ip}\, g^{jq}\, g^{kl}\, (A_{ik} \cdot A_{jl})\, \partial_p X \otimes \partial_q X + 2\, g^{ij}\, g^{kl}\, A_{ik} \otimes A_{jl}.\end{aligned}$$

Proof. Fix a point $p \in M$. We again work in geodesic normal coordinates around p. We compute

$$\begin{aligned}\Delta\pi = {} & g^{ij}\, g^{kl}\, \partial_l A_{ik} \otimes \partial_j X + g^{ij}\, g^{kl}\, \partial_i X \otimes \partial_l A_{jk} \\ & + g^{ij}\, g^{kl}\, A_{ik} \otimes A_{jl} + g^{ij}\, g^{kl}\, A_{il} \otimes A_{jk}\end{aligned}$$

at the point p. Using the Codazzi equations, we obtain

$$(g^{kl}\, \partial_l A_{ik})^\perp = (\partial_i \vec{H})^\perp$$

at p. Moreover,

$$\begin{aligned}\pi(g^{kl}\, \partial_l A_{ik}) &= g^{kl}\, g^{pq}\, (\partial_l A_{ik} \cdot \partial_p X)\, \partial_q X = -g^{kl}\, g^{pq}\, (A_{ik} \cdot \partial_l \partial_p X)\, \partial_q X \\ &= -g^{kl}\, g^{pq}\, (A_{ik} \cdot A_{lp})\, \partial_q X\end{aligned}$$

and

$$\pi(\partial_i \vec{H}) = g^{pq}\,(\partial_i \vec{H} \cdot \partial_p X)\,\partial_q X = -g^{pq}\,(\vec{H} \cdot \partial_i \partial_p X)\,\partial_q X = -g^{pq}\,(\vec{H} \cdot A_{ip})\,\partial_q X$$

at p. Since $g^{kl}\,\partial_l A_{ik} = \pi(g^{kl}\,\partial_l A_{ik}) + (g^{kl}\,\partial_l A_{ik})^\perp$ and $\partial_i \vec{H} = \pi(\partial_i \vec{H}) + (\partial_i \vec{H})^\perp$, we conclude that

$$g^{kl}\,\partial_l A_{ik} = \partial_i \vec{H} + g^{pq}\,(\vec{H} \cdot A_{ip})\,\partial_q X - g^{kl}\,g^{pq}\,(A_{ik} \cdot A_{lp})\,\partial_q X$$

at p. Thus,

$$\begin{aligned}\Delta\pi = {} & g^{ij}\,\partial_i \vec{H} \otimes \partial_j X + g^{ij}\,\partial_i X \otimes \partial_j \vec{H} \\ & + g^{ij}\,g^{pq}\,(\vec{H} \cdot A_{ip})\,\partial_q X \otimes \partial_j X + g^{ij}\,g^{pq}\,(\vec{H} \cdot A_{jp})\,\partial_i X \otimes \partial_q X \\ & - g^{ij}\,g^{kl}\,g^{pq}\,(A_{ik} \cdot A_{lp})\,\partial_q X \otimes \partial_j X - g^{ij}\,g^{kl}\,g^{pq}\,(A_{jk} \cdot A_{lp})\,\partial_i X \otimes \partial_q X \\ & + g^{ij}\,g^{kl}\,A_{ik} \otimes A_{jl} + g^{ij}\,g^{kl}\,A_{il} \otimes A_{jk}\end{aligned}$$

at p. This proves the assertion. ∎

Lemma A.5. *We have*

$$\frac{\partial}{\partial t}\pi - \Delta\pi = 2\,g^{ip}\,g^{jq}\,g^{kl}\,(A_{ik} \cdot A_{jl})\,\partial_p X \otimes \partial_q X - 2\,g^{ij}\,g^{kl}\,A_{ik} \otimes A_{jl},$$

where $\Delta\pi$ denotes the componentwise Laplacian.

Proof. This follows from Lemmas A.2 and A.4. ∎

Lemma A.6. *We have*

$$\frac{\partial}{\partial t}\pi_{\alpha\beta} - \Delta\pi_{\alpha\beta} = 2\sum_\mu g^{kl}\,\partial_k \pi_{\alpha\mu}\,\partial_l \pi_{\beta\mu} - 4\sum_{\mu,\nu} g^{kl}\,\pi_{\mu\nu}\,\partial_k \pi_{\alpha\mu}\,\partial_l \pi_{\beta\nu}.$$

Proof. We compute

$$\sum_\mu g^{kl}\,\partial_k \pi_{\alpha\mu}\,\partial_l \pi_{\beta\mu} = [g^{ij}\,g^{kl}\,A_{ik} \otimes A_{jl} + g^{ip}\,g^{jq}\,g^{kl}\,(A_{ik} \cdot A_{jl})\,\partial_p X \otimes \partial_q X]_{\alpha\beta}$$

and

$$\sum_{\mu,\nu} g^{kl}\,\pi_{\mu\nu}\,\partial_k \pi_{\alpha\mu}\,\partial_l \pi_{\beta\nu} = [g^{ij}\,g^{kl}\,A_{ik} \otimes A_{jl}]_{\alpha\beta}.$$

Hence, the assertion follows from Lemma A.5. ∎

Finally, let us derive the evolution equation for the mean curvature vector $\vec{H}$.

Lemma A.7. *The evolution of the mean curvature is given by*

$$\frac{\partial}{\partial t}\vec{H} - \Delta\vec{H} = 2\,g^{ik}\,g^{jl}\,(\vec{H} \cdot A_{kl})\,A_{ij} + 2\,g^{ij}\,g^{kl}\,(\partial_i \vec{H} \cdot A_{jl})\,\partial_k X,$$

where $\Delta\vec{H}$ denotes the componentwise Laplacian.

Proof. The mean curvature vector is given by

$$\vec{H} = g^{ij}\,\partial_i\partial_j X - g^{ij}\,\Gamma_{ij}^k\,\partial_k X$$

at each point in space-time. Let us fix a point p and work in geodesic normal coordinates around p. In particular, $\Gamma_{ij}^k = 0$ at p. At the point p, we have

$$\frac{\partial}{\partial t}\vec{H} = g^{ij}\,\partial_i\partial_j\Big(\frac{\partial}{\partial t}X\Big) + \frac{\partial}{\partial t}(g^{ij})\,\partial_i\partial_j X - g^{ij}\,\Big(\frac{\partial}{\partial t}\Gamma_{ij}^k\Big)\,\partial_k X.$$

This implies

$$\frac{\partial}{\partial t}\vec{H} - \Delta\vec{H} = 2\,g^{ik}\,g^{jl}\,(\vec{H}\cdot A_{kl})\,A_{ij} - g^{ij}\,\Big(\frac{\partial}{\partial t}\Gamma_{ij}^k\Big)\,\partial_k X$$

at p. We next compute

$$\begin{aligned}
\frac{\partial}{\partial t}\Gamma_{ij}^k &= \frac{1}{2}\,g^{kl}\,\Big(\partial_i\frac{\partial}{\partial t}g_{jl} + \partial_j\frac{\partial}{\partial t}g_{il} - \partial_l\frac{\partial}{\partial t}g_{ij}\Big)\\
&= -g^{kl}\,(\partial_i(\vec{H}\cdot A_{jl}) + \partial_j(\vec{H}\cdot A_{il}) - \partial_l(\vec{H}\cdot A_{ij}))\\
&= -g^{kl}\,((\partial_i\vec{H}\cdot A_{jl}) + (\vec{H}\cdot\partial_i A_{jl}))\\
&\quad - g^{kl}\,((\partial_j\vec{H}\cdot A_{il}) + (\vec{H}\cdot\partial_j A_{il}))\\
&\quad + g^{kl}\,((\partial_l\vec{H}\cdot A_{ij}) + (\vec{H}\cdot\partial_l A_{ij}))
\end{aligned}$$

at p. Consequently,

$$g^{ij}\,\frac{\partial}{\partial t}\Gamma_{ij}^k = -2\,g^{ij}\,g^{kl}\,\partial_i\vec{H}\cdot A_{jl} - 2\,g^{ij}\,g^{kl}\,\vec{H}\cdot\partial_i A_{jl} + 2\,g^{kl}\,\vec{H}\cdot\partial_l\vec{H}$$

at p. Using the Codazzi equations, we obtain $(g^{ij}\,\partial_i A_{jl})^\perp = (\partial_l\vec{H})^\perp$ at p, hence

$$g^{ij}\,\frac{\partial}{\partial t}\Gamma_{ij}^k = -2\,g^{ij}\,g^{kl}\,\partial_i\vec{H}\cdot A_{jl}$$

at p. Putting these facts together, we conclude that

$$\frac{\partial}{\partial t}\vec{H} - \Delta\vec{H} = 2\,g^{ik}\,g^{jl}\,(\vec{H}\cdot A_{kl})\,A_{ij} + 2\,g^{ij}\,g^{kl}\,(\partial_i\vec{H}\cdot A_{jl})\,\partial_k X$$

at p. This proves the assertion. ∎

Lemma A.8. *The evolution of the mean curvature is given by*

$$\frac{\partial}{\partial t}\vec{H}_\alpha - \Delta\vec{H}_\alpha = 2\sum_\beta g^{kl}\,\partial_k\pi_{\alpha\beta}\,\partial_l\vec{H}_\beta + 4\sum_{\beta,\mu} g^{kl}\,\partial_k\pi_{\alpha\mu}\,\partial_l\pi_{\beta\mu}\,\vec{H}_\beta,$$

where $\Delta\vec{H}$ denotes the componentwise Laplacian.

Proof. The identity

$$\sum_{\mu} g^{kl}\,\partial_k \pi_{\alpha\mu}\,\partial_l \pi_{\beta\mu} = [g^{ij}\,g^{kl}\,A_{ik}\otimes A_{jl} + g^{ip}\,g^{jq}\,g^{kl}\,(A_{ik}\cdot A_{jl})\,\partial_p X\otimes\partial_q X]_{\alpha\beta}$$

gives

$$\sum_{\beta,\mu} g^{kl}\,\partial_k \pi_{\alpha\mu}\,\partial_l \pi_{\beta\mu}\,\vec{H}_\beta = [g^{ij}\,g^{kl}\,(\vec{H}\cdot A_{jl})\,A_{ik}]_\alpha.$$

Moreover, using the identity $\partial_l \vec{H}\cdot\partial_j X = -\vec{H}\cdot\partial_l\partial_j X = -\vec{H}\cdot A_{jl}$, we obtain

$$\begin{aligned}\sum_{\beta} g^{kl}\,\partial_k \pi_{\alpha\beta}\,\partial_l \vec{H}_\beta &= [g^{ij}\,g^{kl}\,(\partial_l\vec{H}\cdot A_{jk})\,\partial_i X + g^{ij}\,g^{kl}\,(\partial_l\vec{H}\cdot\partial_j X)\,A_{ik}]_\alpha\\ &= [g^{ij}\,g^{kl}\,(\partial_l\vec{H}\cdot A_{jk})\,\partial_i X - g^{ij}\,g^{kl}\,(\vec{H}\cdot A_{jl})\,A_{ik}]_\alpha.\end{aligned}$$

Hence, the assertion follows from Lemma A.7. ∎

Acknowledgements. The authors wish to deeply thank Simon Brendle for bringing this topic to their attention as well as for his fundamental ideas, particularly his contributions to deriving the evolution equations presented in Appendix A.

Funding. The work of Balázs Kovács is funded by the Heisenberg Programme of the Deutsche Forschungsgemeinschaft (DFG, German Research Foundation) with Project-ID 446431602.

References

[1] G. Akrivis, M. Chen, F. Yu, and Z. Zhou, The energy technique for the six-step BDF method. *SIAM J. Numer. Anal.* **59** (2021), no. 5, 2449–2472 Zbl 1483.65153 MR 4316580

[2] G. Akrivis, B. Li, and C. Lubich, Combining maximal regularity and energy estimates for time discretizations of quasilinear parabolic equations. *Math. Comp.* **86** (2017), no. 306, 1527–1552 Zbl 1361.65053 MR 3626527

[3] S. J. Altschuler, Singularities of the curve shrinking flow for space curves. *J. Differential Geom.* **34** (1991), no. 2, 491–514 Zbl 0754.53006 MR 1131441

[4] S. J. Altschuler and M. A. Grayson, Shortening space curves and flow through singularities. *J. Differential Geom.* **35** (1992), no. 2, 283–298 Zbl 0782.53001 MR 1158337

[5] L. Ambrosio and H. M. Soner, Flow by mean curvature of surfaces of any codimension. In *Variational methods for discontinuous structures (Como, 1994)*, pp. 123–134, Progr. Nonlinear Differential Equations Appl. 25, Birkhäuser, Basel, 1996 Zbl 0878.35053 MR 1414495

[6] L. Ambrosio and H. M. Soner, Level set approach to mean curvature flow in arbitrary codimension. *J. Differential Geom.* **43** (1996), no. 4, 693–737 Zbl 0868.35046 MR 1412682

[7] B. Andrews and C. Baker, Mean curvature flow of pinched submanifolds to spheres. *J. Differential Geom.* **85** (2010), no. 3, 357–395 Zbl 1241.53054 MR 2739807

[8] S. Angenent, Formal asymptotic expansions for symmetric ancient ovals in mean curvature flow. *Netw. Heterog. Media* **8** (2013), no. 1, 1–8 Zbl 1267.53065 MR 3043925

[9] J. W. Barrett, H. Garcke, and R. Nürnberg, On the parametric finite element approximation of evolving hypersurfaces in $\mathbb{R}^3$. *J. Comput. Phys.* **227** (2008), no. 9, 4281–4307 Zbl 1145.65068 MR 2406538

[10] J. W. Barrett, H. Garcke, and R. Nürnberg, Numerical approximation of gradient flows for closed curves in $\mathbb{R}^d$. *IMA J. Numer. Anal.* **30** (2010), no. 1, 4–60 Zbl 1185.65027 MR 2580546

[11] J. W. Barrett, H. Garcke, and R. Nürnberg, Parametric approximation of isotropic and anisotropic elastic flow for closed and open curves. *Numer. Math.* **120** (2012), no. 3, 489–542 Zbl 1242.65188 MR 2890298

[12] S. Bartels, C. Carstensen, and A. Hecht, P2Q2Iso2D=2D isoparametric FEM in Matlab. *J. Comput. Appl. Math.* **192** (2006), no. 2, 219–250 Zbl 1091.65112 MR 2228811

[13] T. Binz and B. Kovács, A convergent finite element algorithm for generalized mean curvature flows of closed surfaces. *IMA J. Numer. Anal.* **42** (2022), no. 3, 2545–2588 Zbl 07563202 MR 4454930

[14] E. Carlini, M. Falcone, and R. Ferretti, A semi-Lagrangian scheme for the curve shortening flow in codimension-2. *J. Comput. Phys.* **225** (2007), no. 2, 1388–1408 Zbl 1255.65157 MR 2349186

[15] K. Deckelnick and G. Dziuk, On the approximation of the curve shortening flow. In *Calculus of variations, applications and computations (Pont-à-Mousson, 1994)*, pp. 100–108, Pitman Res. Notes Math. Ser. 326, Longman Scientific & Technical, Harlow, 1995 Zbl 0830.65096 MR 1419337

[16] K. Deckelnick, G. Dziuk, and C. M. Elliott, Computation of geometric partial differential equations and mean curvature flow. *Acta Numer.* **14** (2005), 139–232 Zbl 1113.65097 MR 2168343

[17] A. Demlow, Higher-order finite element methods and pointwise error estimates for elliptic problems on surfaces. *SIAM J. Numer. Anal.* **47** (2009), no. 2, 805–827 Zbl 1195.65168 MR 2485433

[18] W. Dörfler and R. Nürnberg, Discrete gradient flows for general curvature energies. *SIAM J. Sci. Comput.* **41** (2019), no. 3, A2012–A2036 Zbl 1434.65178 MR 3968254

[19] G. Dziuk, Finite elements for the Beltrami operator on arbitrary surfaces. In *Partial differential equations and calculus of variations*, pp. 142–155, Lecture Notes in Math. 1357, Springer, Berlin, 1988 MR 976234

[20] G. Dziuk, An algorithm for evolutionary surfaces. *Numer. Math.* **58** (1991), no. 6, 603–611 Zbl 0714.65092 MR 1083523

[21] G. Dziuk, Convergence of a semi-discrete scheme for the curve shortening flow. *Math. Models Methods Appl. Sci.* **4** (1994), no. 4, 589–606 Zbl 0811.65112 MR 1291140

[22] G. Dziuk and C. M. Elliott, Finite elements on evolving surfaces. *IMA J. Numer. Anal.* **27** (2007), no. 2, 262–292 Zbl 1120.65102 MR 2317005

[23] G. Dziuk and C. M. Elliott, Finite element methods for surface PDEs. *Acta Numer.* **22** (2013), 289–396 Zbl 1296.65156 MR 3038698

[24] C. M. Elliott and V. Styles, An ALE ESFEM for solving PDEs on evolving surfaces. *Milan J. Math.* **80** (2012), no. 2, 469–501 Zbl 1259.65147 MR 3000495

[25] E. Hairer and G. Wanner, *Solving ordinary differential equations. II*. Second edn., Springer Ser. Comput. Math. 14, Springer, Berlin, 1996 Zbl 0859.65067 MR 1439506

[26] G. Huisken, Flow by mean curvature of convex surfaces into spheres. *J. Differential Geom.* **20** (1984), no. 1, 237–266 Zbl 0556.53001 MR 772132

[27] B. Kovács, High-order evolving surface finite element method for parabolic problems on evolving surfaces. *IMA J. Numer. Anal.* **38** (2018), no. 1, 430–459 Zbl 1406.65086 MR 3800028

[28] B. Kovács, B. Li, and C. Lubich, A convergent evolving finite element algorithm for mean curvature flow of closed surfaces. *Numer. Math.* **143** (2019), no. 4, 797–853 Zbl 1427.65250 MR 4026373

[29] B. Kovács, B. Li, and C. Lubich, A convergent algorithm for forced mean curvature flow driven by diffusion on the surface. *Interfaces Free Bound.* **22** (2020), no. 4, 443–464 Zbl 1458.35016 MR 4184582

[30] B. Kovács, B. Li, and C. Lubich, A convergent evolving finite element algorithm for Willmore flow of closed surfaces. *Numer. Math.* **149** (2021), no. 3, 595–643 Zbl 1496.65165 MR 4344594

[31] B. Kovács, B. Li, C. Lubich, and C. A. P. Guerra, Convergence of finite elements on an evolving surface driven by diffusion on the surface. *Numer. Math.* **137** (2017), no. 3, 643–689 Zbl 1377.65131 MR 3712288

[32] B. Li, Convergence of Dziuk's semidiscrete finite element method for mean curvature flow of closed surfaces with high-order finite elements. *SIAM J. Numer. Anal.* **59** (2021), no. 3, 1592–1617 Zbl 1479.65008 MR 4269969

[33] C. Lubich, D. Mansour, and C. Venkataraman, Backward difference time discretization of parabolic differential equations on evolving surfaces. *IMA J. Numer. Anal.* **33** (2013), no. 4, 1365–1385 Zbl 1401.65108 MR 3119720

[34] S. Lynch and H. T. Nguyen, Pinched ancient solutions to the high codimension mean curvature flow. *Calc. Var. Partial Differential Equations* **60** (2021), no. 1, paper no. 29 Zbl 1458.53099 MR 4201652

[35] K. Mikula and J. Urbán, A new tangentially stabilized 3D curve evolution algorithm and its application in virtual colonoscopy. *Adv. Comput. Math.* **40** (2014), no. 4, 819–837 Zbl 1296.65030 MR 3240215

[36] K. Naff, A planarity estimate for pinched solutions of mean curvature flow. *Duke Math. J.* **171** (2022), no. 2, 443–482 Zbl 1494.53102 MR 4375620

[37] P. Pozzi, Anisotropic curve shortening flow in higher codimension. *Math. Methods Appl. Sci.* **30** (2007), no. 11, 1243–1281 Zbl 1122.65081 MR 2334978

[38] P. Pozzi, Anisotropic mean curvature flow for two-dimensional surfaces in higher codimension: a numerical scheme. *Interfaces Free Bound.* **10** (2008), no. 4, 539–576 Zbl 1158.65076 MR 2465273

[39] K. Smoczyk, Mean curvature flow in higher codimension: introduction and survey. In *Global differential geometry*, pp. 231–274, Springer Proc. Math. 17, Springer, Heidelberg, 2012 Zbl 1247.53004 MR 3289845

[40] M.-T. Wang, Mean curvature flows in higher codimension. In *Second International Congress of Chinese Mathematicians*, pp. 275–283, New Stud. Adv. Math. 4, International Press, Somerville, MA, 2004 Zbl 1328.53091 MR 2497990

[41] M.-T. Wang, Lectures on mean curvature flows in higher codimensions. In *Handbook of geometric analysis. No. 1*, pp. 525–543, Adv. Lect. Math. (ALM) 7, International Press, Somerville, MA, 2008 Zbl 1167.53058 MR 2483374

Received 2 February 2022; revised 10 January 2023.

Tim Binz
Department of Mathematics, TU Darmstadt, Schlossgartenstraße 7, 64289 Darmstadt, Germany;
binz@mathematik.tu-darmstadt.de

Balázs Kovács
Faculty of Mathematics, University of Regensburg, Universitätsstraße 31, 93053 Regensburg, Germany; balazs.kovacs@mathematik.uni-regensburg.de